# Synthesis and Characterization of Poly(butyl acrylate)/Silica and Poly(butyl acrylate)/Silica/Poly(methyl methacrylate) Composite Particles

**Dong-Ming Qi, Yong-Zhong Bao, Zhi-Ming Huang, Zhi-Xue Weng**

*State Key Laboatory of Polymer Reaction Engineering, Zhejiang University, Hangzhou, 310027, China*

**ABSTRACT:** Poly(butyl acrylate)/poly(methyl methacrylate) (PBA/PMMA) core–shell particles embedded with nanometer-sized silica particles were prepared by emulsion polymerization of butyl acrylate (BA) in the presence of silica particles preabsorbed with 2,2'-azobis(2-amidinopropane)dihydrochloride (AIBA) initiator and subsequent MMA emulsion polymerization in the presence of PBA/silica composite particles. The morphologies of the resulting PBA/silica and PBA/silica/PMMA composite particles were characterized, which showed that AIBA could be absorbed effectively onto silica particles when the pH of the dispersion medium was greater than the isoelectric potential point of silica. The critical amount of AIBA added to have stable dispersion of silica particles increased as the pH of the dispersion medium increased. PBA/silica composite particles prepared by *in situ* emulsion polymerization using silica preabsorbed with AIBA showed higher silica absorption efficiency than did the PBA/silica composite particles prepared by direct mixing of PBA latex and silica dispersion or by emulsion polymerization in which AIBA was added after the mixing of BA and silica. The PBA/silica composite particles exhibited a raspberrylike morphology, with silica particles "adhered" to the surfaces of the PBA particles, whereas the PBA/silica/PMMA composite latex particles exhibited a sandwich morphology, with silica particles mainly at the interface between the PBA core and the PMMA shell. Subsequently, the PBA/silica/PMMA composite latex obtained had a narrow particle size distribution and good dispersion stability. © 2006 Wiley Periodicals, Inc. J Appl Polym Sci 99: 3425–3432, 2006

**Key words:** emulsion polymerization; nanocomposite; morphology; core-shell polymers

## INTRODUCTION

During the past two decades, there has been significant work directed toward the elaboration of nanocomposite particles by embedding inorganic particles in the polymer matrix.[1–3] These materials combine the properties of inorganic particles (in terms of mechanical strength, modulus, and thermal stability) with the processability and flexibility of organic polymer matrix. Because direct melt-mixing of polymer with inorganic components would not achieve good dispersion of inorganic particles in the polymer matrix or provide acceptable interfacial adhesion between the polymer and inorganic particles, much attention has been paid to the synthesis of polymer nanocomposites using various chemical processes such as conducting polymerization in the presence of inorganic particles.[4–6]

Many researchers have performed vinyl monomer polymerization in the presence of nanometer silica ($SiO_2$) particles in order to prepare polymer/$SiO_2$ nanocomposites with enhanced interface adhesion. Furusawa et al.[7] prepared a polystyrene/silica composite by conducting polymerization in the presence of silica adsorbed with a dense layer of hydroxypropyl cellulose. Boutgeat-Lami et al.[8–10] grafted methacryloylpropyltrimethoxysilane (MPTMS) as a coupling agent on the surface of silica and carried out ethyl acrylate emulsion polymerization in the presence of modified silica. Zhang et al.[11] treated the silica by the same method and prepared monodispersed silica–polystyrene core–shell microspheres by *in situ* emulsion polymerization. Hajji et al.[12,13] prepared poly(2-hydroxyethyl methacrylate)/silica nanocomposites by conducting the polymerization in the presence of HEMA-functionalized silica nanoparticles.

Hayashi et al.[14] anchored peroxide groups on the surface of silica particles by a Michael addition and then initiated the free-radical polymerization of vinyl monomers from the modified particles. Carrot et al.[15] bound the atom transfer radical polymerization initiator to silica nanoparticles and carried out butyl acrylate polymerization from modified particles.

TABLE I
Polymerization Recipes for Conventional and *In Situ* Emulsion Polymerizations of BA

| Ingredients (g) | No. 1a PBA + AIBA | No. 2a PBA + KPS | No. 3 SiO₂ anchored with AIBA + OP + BA | No. 4 Pure SiO₂ + OP + (AIBA + BA) |
|---|---|---|---|---|
| $H_2O$ (pH = 10) | 90 | 90 | 92 | 92 |
| Silica aqueous dispersion | — | — | 4.0 | 4.0 |
| OP-10 surfactant | 0.15 | 0.15 | 0.1 | 0.1 |
| BA monomer | 6.0 | 6.0 | 4.0 | 4.0 |
| EGDMA crosslinker | 0.061 | 0.058 | 0.041 | 0.039 |
| Initiator | | | | |
| AIBA | 0.033 | / | 0.032 | 0.032 |
| KPS | — | 0.024 | — | — |

Barthet et al.[16,17] applied the strong acid–base interaction between 4-vinylpyridine and silica to form nanocomposite particles in a surfactant-free system. Bourgeat-Lami and Lang[18,19] synthesized polymer-encapsulated silica particles using dispersion polymerization of styrene in an aqueous ethanol medium using poly(*N*-vinyl pyrrolidone) (PVP) as a stabilizer. Luna-Xavier et al.[20–22] found that the presence of electrostatic attraction between silica and an initiator was crucial to achieving a mixed polymer/silica structure, whose coarse surface looked like raspberries.
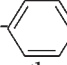
A core–shell structured acrylic polymer (ACR) with a rubberlike polymer core is widely used as an impact modifier for general purpose plastics such as poly(vinyl chloride) and poly(methyl methacrylate). Incorporation of inorganic nanoparticles in ACR is a useful way to simultaneously increase the stiffness and toughness of the modified plastics.[23,24]

In the present study, poly(butyl acrylate)/poly(methyl methacrylate) (PBA/PMMA) core–shell particles embedded with nanometer-sized silica particles were prepared by *in situ* emulsion polymerization in the presence of silica particles anchored with an azo initiator, and the structure of the composite particles was characterized.

## EXPERIMENTAL

### Materials

Commercial butyl acrylate (BA) and methyl methacrylate (MMA) were distilled under reduced pressure before polymerization. Silica aqueous dispersion (30 wt % solid content) was supplied by Zhoushan Mingri Nanometer Material Co. (Zhoushan, China). The size of silica particles was between 10 and 15 nm, determined by a laser electrophoresis with a zeta potential analyzer (Zetasizer 3000HS; Malvern Instruments, Laramie, WY) and by transmission electron microscopy (TEM; JEOL JSM-1230EX T20, Tokyo, Japan). 2.2'-Azobis(2-amidinopropane)dihydrochloride (AIBA) and potassium persulfate (KPS) with analytical purity were obtained from Across

Organics Co. (Geel, Belgium). Nonionic surfactant nonylphenol poly(oxyethylene)($C_9H_{19}$-⟨phenyl⟩-(OOCH₂-CH₂)₁₀-OH, OP-10) and ethyl glycol dimethacrylate (EGDMA), used as a crosslinker, were purchased from Anli Chemical Factory (Suzhou, China). Ammonia and hydrochloric acid were used as received.

### Preparation of PBA/silica/PMMA composite latex particles

Adsorption of AIBA initiator onto silica particles

The adsorption of AIBA onto silica particles at different pHs was performed in a nitrogen atmosphere. The adsorption isotherm was determined by mixing silica dispersion and AIBA aqueous solution with different ratios of pure silica and AIBA in a capped glass vessel at 25°C. The mixed dispersion was agitated using a magnetic stirrer at ambient temperature for 10 min. Then the dispersion was centrifuged at 15,000 rpm for 30 min. The initiator concentration in the serum was
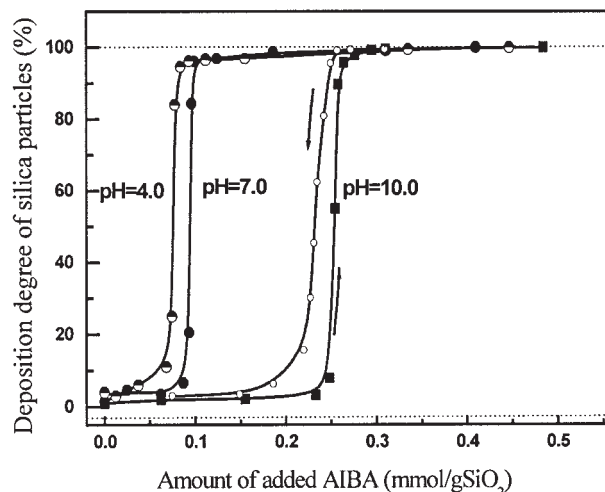


**Figure 1** Variation in degree of deposition of silica with AIBA/SiO₂ ratio at different pHs of medium.
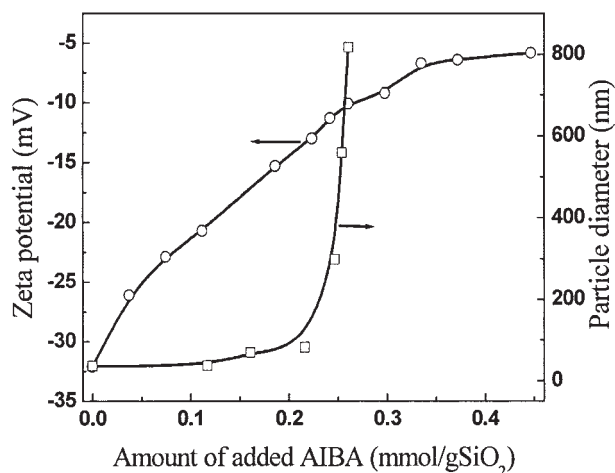
**Figure 2** Variation in zeta potential and diameter of silica particles with AIBA/SiO$_2$ ratio at pH 10.



**Figure 3** Absorption of isotehms of AIBA on silica particles at pH 10.

determined by UV spectroscopy analysis using an UV–vis spectrophotometer (UV751GD). A calibration curve was established to determine the initiator concentration in serum without silica. The amount of adsorbed initiator was calculated from the difference between the total amount of initiator added and the amount of initiator in the serum.

### Preparation of PBA/silica composite latex particles

PBA/silica composite latex particles were prepared using two methods: (1) mixing of silica dispersion with preprepared PBA latex and (2) conducting BA emulsion polymerization in the presence of silica particles.

Two PBA latices were synthesized using conventional emulsion polymerization methods, the AIBA and KPS initiator methods. A 200-mL glass reactor fitted with a condenser, an N$_2$ inlet, a thermometer, and a paddle-type agitator was charged with deionized water, BA, and nonionic surfactant OP-10. The mixture was gently agitated for 1 h at ambient temperature. Then a certain amount of AIBA or KPS solution was added when the temperature of the mixture in the reactor reached 70°C, allowing the polymerization of BA. The polymerization lasted for 5 h under an N$_2$ atmosphere. The detailed procedures for the preparation of the two kinds of PBA latices, numbers 1a and 2a, are shown in Table I. PBA/silica composite latices were obtained by adding silica dispersion (with 4.0 g of silica) to PBA latices 1a and 2a and mixing for 180 min at 70°C. The obtained composite latices were marked as 1b and 2b.

Using a batch process, BA emulsion polymerization in the presence of silica was conducted in the same reactor. The reactor was charged with deionized water, the original silica dispersion or a dispersion of the
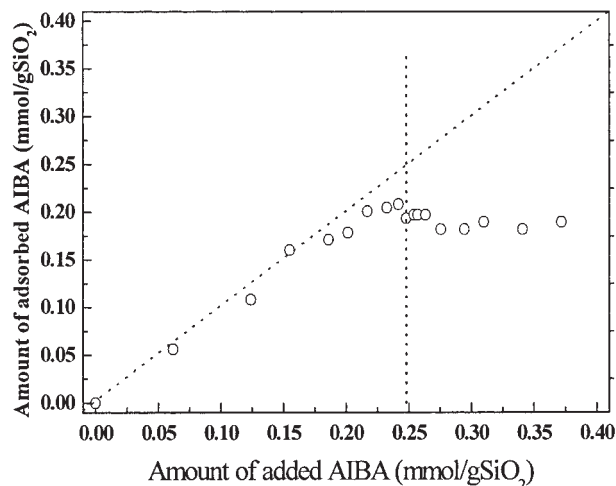
silica anchored with AIBA, and nonionic surfactant OP-10. The mixture was gently agitated for 1 h at ambient temperature. Then BA (or BA and AIBA with the pure silica dispersion) was added to initiate the polymerization at 70°C under an N$_2$ atmosphere. Detailed instructions for the polymerization are shown in Table I, and the composite latex particles are numbered 3 and 4.

### In situ polymerization of MMA in the presence of PBA/silica composite latex

First, 10 g of deionized water, 0.1 g of OP-10, 0.032 g of AIBA, and 4.5 g of MMA were added to PBA/silica composite latex 3 (100 g). Emulsion polymerization of MMA in the presence of PBA/silica composite parti-
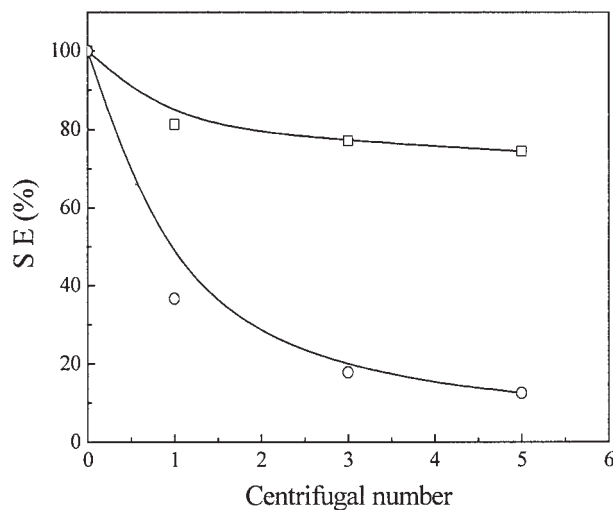


**Figure 4** Variation of adsorbed efficiency of silica with centrifugal/redispersion cycles: (○) sample 1b; (□) sample 3.

**TABLE II**
**Characteristics of PBA Latex Particles and PBA/Silica Composite Latex Particles**

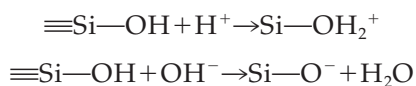| Sample No. | Size (nm)[a] | $D_w/D_n$ | Zeta potential (mv)[b] | SE |
|---|---|---|---|---|
| a | 213 | 1.01 | 19.7 | — |
| 2a | 237 | 1.02 | −21.3 | — |
| 1b | 224 | 1.04 | 12.7 | 36.7% |
| 2b | 230 | 1.05 | −18.5 | 12.5% |
| 3 | 250 | 1.03 | −29.7 | 81.3% |
| 4 | 310 | 1.08 | −26.2 | 54.2% |

[a] Measured by DLS; [b] pH = 10.

cles was carried out at 70°C for up to 5 h under an $N_2$ atmosphere in order to obtain PBA/silica/PMMA composite particles.
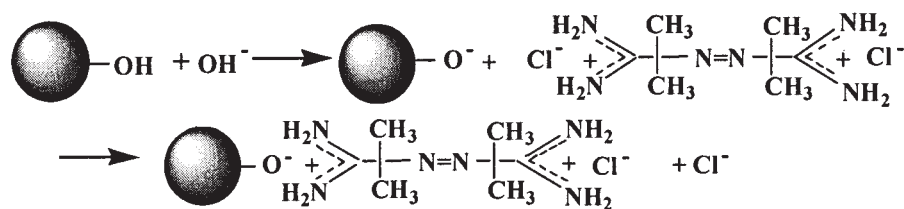
## Characterization

The average size and zeta potential of the silica particles in the dispersion with different AIBA concentrations were determined by dynamic light scattering (Zetasizer 3000HS, Malvern Instruments, Laramie, WY). The deposition stabilization of the silica dispersion with different AIBA concentrations was determined gravimetrically.

Silica adsorption efficiency, SE, was defined as the ratio of the amount of silica in the composite particles to the total amount of silica added. The amount of silica in the composite particles was calculated from the total amount of added silica and the amount of silica in the serum after the product was centrifuged at 15,000 rpm for 30 min.

The average size of the PBA/silica and PBA/silica/PMMA composite latex particles was determined by dynamic light scattering (Zetasizer 3000HS, Malvern Instruments, Laramie, WY). The morphology of composite particles was observed with a transmission electron microscope (TEM-1230EX, JEOL Co., Tokyo, Japan).

The polymerization conversions were determined gravimetrically. The polymer content in the composite particles was determined by thermogravimetric analysis of the composite particles. Thermal analysis experiments were carried out using a TGA analyzer (Perkin-Elmer Pyris, Wellesley, MA) by heating the sample (10 mg) in air with a temperature gradient from ambient temperature to 700°C increasing at a rate of 10°C/min.

## RESULTS AND DISCUSSION

### Adsorption of AIBA initiator onto silica particles

The effective absorption of AIBA onto the surface of silica particles is a key factor affecting the "grafting" polymerization of BA or MMA monomer from the surface of silica particles and the content of polymer in the composite particles. Thus, it is important to obtain optimized absorption conditions before carrying out polymerization.

The hydration reaction of $SiO_2$ in water is

$$\equiv Si—OH + H^+ \rightarrow Si—OH_2^+ \quad pH < isoelectric potential$$

$$\equiv Si—OH + OH^- \rightarrow Si—O^- + H_2O \quad pH > isoelectric potential$$

The isoelectric potential (IEP) of $SiO_2$ particles is 1.5–3.7.[6] So silica particles would exhibit a negative charge when the pH value of the dispersion medium was greater than 3.7. The measured zeta potential of silica particles was −32.1 mv in dispersion at a concentration of 1.2 wt % and a pH of 10. The measured zeta potential of the AIBA aqueous solution (0.1 wt %) was 13.0 mv. Thus, AIBA was easily absorbed onto silica particles through the following mechanism:



Silica particles exhibit different charge properties at different pHs of the dispersion medium, and charge properties would be changed as AIBA initiator was added. As a result, the dispersion stability would be changed as the pH and the amount of added AIBA varied. The effect of the AIBA/silica ratio and the pH of the medium on the degree of deposition of silica particles after high-speed centrifugation is shown in Figure 1.

It can be seen that the degree of deposition of silica particles increased slowly with the increase of the AIBA/silica ratio when the amount of AIBA added
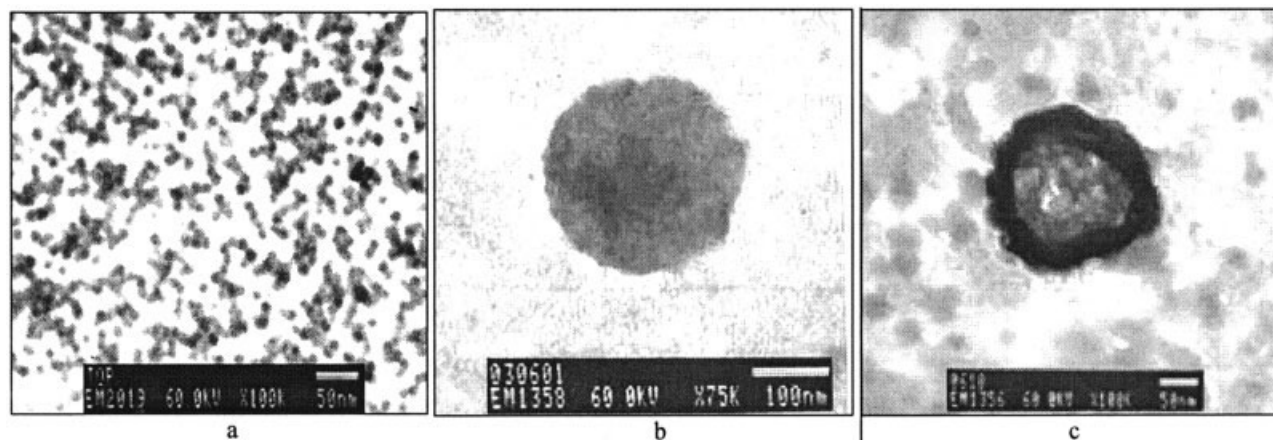
**Figure 5**   TEM micrographs of (a) $SiO_2$, (b) PBA latex, and (c) PBA/silica composite 3.

was lower but increased rapidly when AIBA/silica ratio exceeded a critical value. The critical AIBA/silica ratio for stable dispersion of silica increased with an increase of the pH. The silica particles exhibited a negative charge when the pH was greater than the IEP of silica, and the amount of net charge on the silica surface increased with an increasing pH of the medium because of the enhancement of silica hydration. The absorption between silica particles and AIBA occurred because of the electrostatic attraction between them, and the amount of net charge on the silica surface gradually decreased as more and more AIBA was absorbed. When the added amount of AIBA was close to a critical value, the net charge of the silica particles was close to zero; thus, the electrostatic repulsive force between the silica particles was not great enough to resist the centrifugal force. Inevitably, aggregation of the silica particles occurred. Therefore, there is a critical amount of added AIBA for the stable dispersion of silica particle at a given pH, and this critical value increases with an increasing pH. From the result shown in Figure 1, it can be seen that the critical amount of added AIBA was 0.208 mmol/g $SiO_2$ at pH 10.

Variations in the zeta potential and particle size of the silica with the AIBA/silica ratio at pH 10.0 are shown in Figure 2. It can be seen that the zeta potential gradually increased as the amount of added AIBA increased. The particle size of the silica increased slowly when the amount of added AIBA was lower but increased rapidly when the amount of added AIBA exceeded the critical amount.

Variation in the amount of adsorbed AIBA initiator on the silica with the amount of added AIBA at pH 10 is shown in Figure 3. It can be seen that almost all AIBA initiator was adsorbed onto the silica particles when the amount of added AIBA was lower. Then the amount of adsorbed AIBA reached a plateau with an equilibrium absorption of about 0.18 mmol/g $SiO_2$.

The higher percentage of AIBA absorbed on the surface of the silica would favor formation of polymer/silica composite particles with a higher percentage of "grafted" polymer. Thus, 0.10 mmol AIBA/$gSiO_2$ was added to prepare particles of PBA/silica composite latex 3.

## Preparation of PBA/silica composite latex particles

The volume average particle size, particle size distribution index ($D_w/D_n$), zeta potential of PBA latex particles and PBA/silica composite latex particles, and SE for composite latex particles are shown in Table II.

It can be seen that the particle sizes of the two PBA latices (Nos. 1a and 2a), the two PBA/silica composite latices prepared by direct mixing (Nos. 1b and 2b), and PBA/silica composite latex 3 ranged from 213 to 250 nm, whereas the particle size of PBA/silica com-
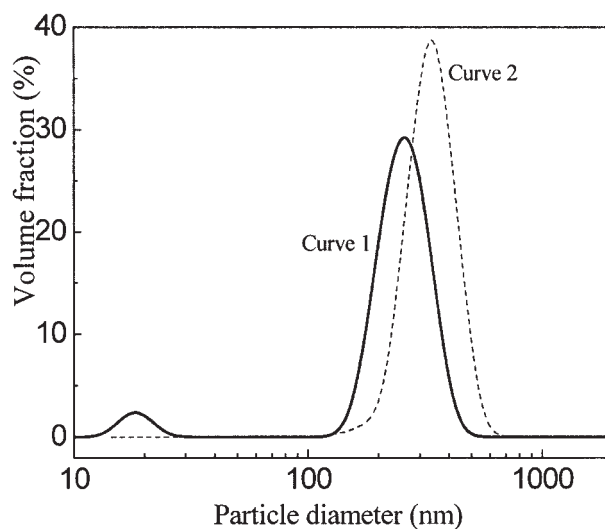


**Figure 6**   Size distribution of PBA/$SiO_2$ (curve 1) and PBA/$SiO_2$/PMMA (curve 2) composite particles.
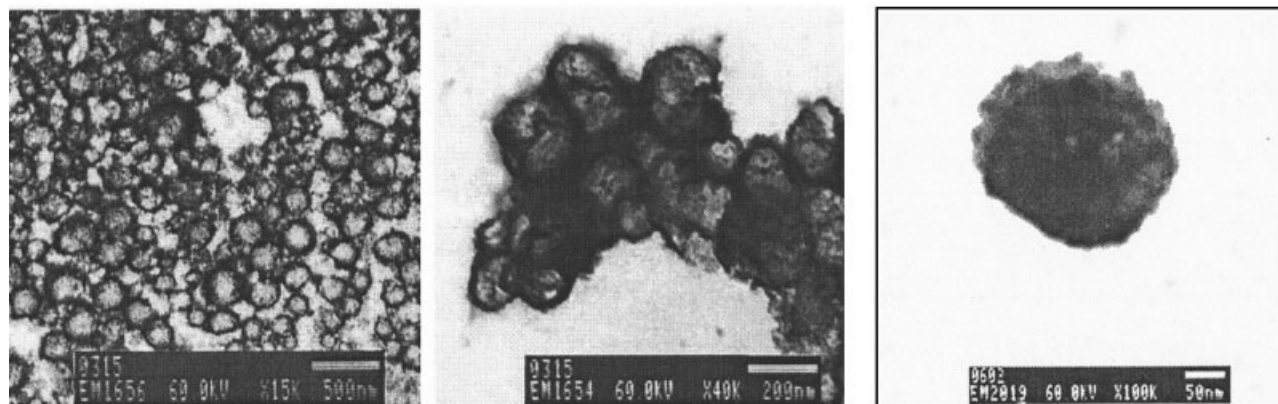
**Figure 7**  TEM micrographs of PBA/SiO$_2$/PMMA composite particles.

posite latex 4 was greater than 300 nm. The particle size distributions were narrow for all PBA and PBA/silica composite latices.

In the deposition experiment, no deposition was found when silica dispersion was centrifuged, whereas nearly all PBA latex particles prepared by using either AIBA or KPS as the initiator were deposited. It can be seen from Table II that the SE of the PBA/silica composite latex particles prepared from the direct mixing of silica dispersion and PBA 1a was 36.7%, whereas it was just 12.5% when PBA latex 2a was used in mixing. Electrostatic attraction was considered the main force prompting the combining of the PBA and the silica particles in the direct-mixing process. The electrostatic attraction between silica and PBA particles in the PBA latex 1a particles and the silica particles was shown by the former exhibiting positive zeta potential and the latter exhibiting negative zeta potential. However, because both the PBA latex 2 particles and silica particles exhibited a negative zeta, it was difficult for silica to be absorbed onto the PBA particles.

By comparing the SE of particles of PBA/silica composite 3 with that of particles of PBA/silica composite 4, it can be seen that the sequential addition of AIBA and OP-10 surfactant had a great influence on the SE of the composite particles. A smaller SE was achieved when AIBA was added after the surfactant. This was caused by the competitive absorption of AIBA initiator and OP-10 surfactant onto the silica surface.[22] A

hydrate layer would be formed on the surface of silica when surfactant was added first; then it became difficult for AIBA to penetrate through the hydrate layer. The best result, that is, 81.3% of silica particles absorbed onto the PBA particles, was obtained when AIBA initiator was absorbed onto silica particles before polymerization. With this method, most AIBA molecules were selectively adsorbed onto the bare silica surface because of electrostatic attraction, and therefore the absorbed AIBA would initiate BA polymerization from the surface of the silica particles.

To evaluate the combination of silica and PBA, particles of PBA/silica composites 1b and 3 were separated from the dispersion medium by centrifugation and then were dispersed in water whose pH was 10 through magnetic stirring. This process was repeated several times. The variation in SE with centrifugal/dispersion cycles is shown in Figure 4. It can be seen that the SE of sample 3 was much higher than that of sample 1b. Most of the silica particles remained stably combined with PBA particles after repeated processing.

### Morphology of PBA/silica composite particles

TEM micrographs of silica, PBA latex, and PBA/silica composite particles are shown in Figure 5. It can be seen from Figure 5(c) that the composite particles had a raspberrylike morphology, with silica particles absorbed onto the surface of PBA particles. In addition to

**TABLE III**
**Comparison on the Size of Composite Particles Using Various Methods**

| Composite particles | Measure by DLS | Determined from TEM | Calculated using weight ratio from | |
|---|---|---|---|---|
| | | | Gravimetric method | TGA analysis |
| PBA/SiO$_2$ | 250nm | 230nm | — | — |
| PBA/SiO$_2$/PMMA | 320nm | 285nm | 301 | 303 |

the absorbed silica particles, there were some free silica particles in continuous phase, findings in agreement with those of the quantitative analysis shown in Table II.

There are two possible reasons for the distribution of silica on the surface of PBA. The first is that small silica particles are easy to adsorb onto the surface of big PBA particles through physical adsorption. The other is that the polarity of silica particles lies between those of BA and water. According to Pickering stabilizer theory,[25] silica particles tend to enrich at the oil–water interface.

## Morphology and composition of PBA/silica/PMMA composite particles

Using PBA/silica composite latex 3 as the seeds, MMA emulsion polymerization was carried out in order to prepare PBA/SiO$_2$/PMMA composite latex particles. The particle size distributions of the PBA/silica and PBA/silica/PMMA composite latices are shown in Figure 6.

It can be seen that the particle size distributions of the PBA/silica and PBA/silica/PMMA composite latices were narrow and that the distribution peak of PBA/silica composite particles became greater in size as MMA polymerized. The volume average diameter increased from 250 nm for the PBA/silica composite particles to 320 nm for the PBA/silica/PMMA composite particles, as measured by DLS. The distribution peak of the free silica particles vanished, and no new small-sized peak appeared after MMA polymerization.

Typical TEM micrographs of PBA/silica/PMMA composite particles are shown in Figure 7. In com-

**TABLE IV**
**Weight Percent of Main Components of PBA/silica/PMMA Composite Particles**

| Layer | Conversion (%) | Weight percent of main components in composite particles (%) | |
| --- | --- | --- | --- |
| | | Gravimetry | TGA analysis |
| PBA | 82.6 | 47.67 | 47.75 |
| SiO$_2$ | 100 | 11.53 | 10.35 |
| PMMA | 78.3 | 40.80 | 41.90 |

parison with the micrograph of PBA/silica composite shown particles in Figure 5(c), it can be seen that a well shell layer was formed to coat the silica layer and that there were no free silica particles in the continuous phase as MMA polymerized. It was confirmed that the silica particles absorbed on the surface of PBA particles had been encapsulated by the PMMA layer, and free silica particles had been combined with composite particles. It can also be seen that the surface of PBA/silica/PMMA composite particles was still coarse. This is possibly because of the direct polymerization of MMA on the surface of PBA/silica composite particles, resulting in the coagulation of bigger PBA/silica composite particles with smaller PMMA/silica composite particles, which were formed through MMA polymerization initiated by AIBA absorbed onto the residual free silica particles.

The diameters of the PBA/SiO$_2$/PMMA and PBA/SiO$_2$ composite particles determined by DLS and TEM micrographs are listed in Table III. In addition, presuming the number of composite particles to be constant, the diameter of PBA/SiO$_2$/PMMA latex (D$_2$) can be calculated from the weight change of the composite particles by this equation:

$$\frac{D_2}{D_1} = \left(\frac{V_2}{V_1}\right)^{1/3} \approx \left(\frac{W_2}{W_1}\right)^{1/3} \tag{1}$$

where the diameter of PBA/SiO$_2$ latex (D$_1$) is 250 nm, measured by DLS, $W_2/W_1$ is the weight ratio of PBA/SiO$_2$/PMMA to PBA/SiO$_2$ composite particles, which can be determined by gravimetric or TGA analysis. The calculated results are also listed in Table III for comparison.

From the above comparison, it can be seen that the diameter of PBA/SiO$_2$/PMMA latex particles obtained from direct observation was close to the theoretical calculation, supporting that MMA polymerization mainly occurred on the surface of the PBA/silica particles. This process is illustrated as follows:
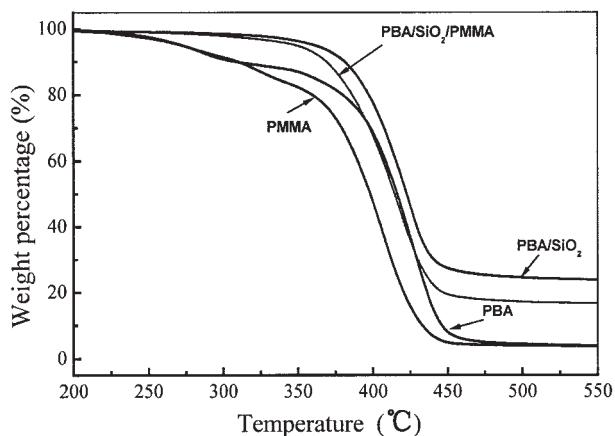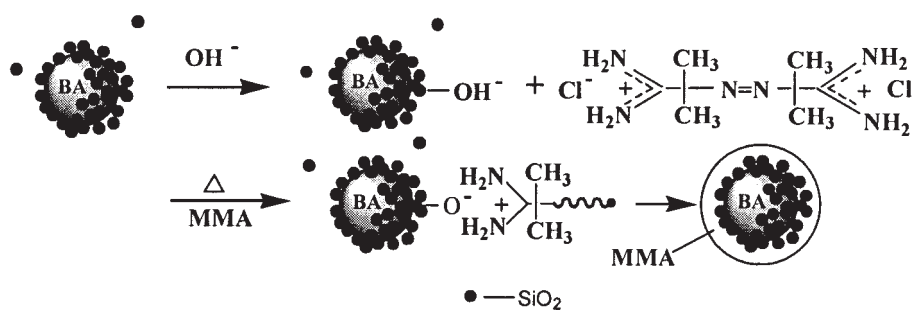
**Figure 8** TGA curves of PBA, PMMA, PBA/SiO$_2$, and PBA/SiO$_2$/PMMA particles.

Typical TGA curves of the PBA, PMMA, PBA/SiO$_2$, and PBA/SiO$_2$/PMMA samples are shown in Figure 8. Comparing the weight loss percentage of organic and inorganic compounds, the weight percent of the main components were calculated and are shown in Table IV. It can be seen that the weight percent of PBA, silica, and PMMA composition determined by the weighing method and TGA analysis fit well.

## CONCLUSIONS

AIBA could be effectively absorbed onto silica particles when the pH of the dispersion medium was greater than the isoelectric potential point of the silica. The critical amount of AIBA necessary to be added for the stable dispersion of the silica particles increased as the pH of the dispersion medium increased. The PBA/silica composite latex particles that had higher silica absorption efficiency (81.3%) were prepared by BA emulsion polymerization in the presence of silica particles with absorbed AIBA. The PBA/silica composite particles obtained exhibited a raspberrylike morphology with silica particles absorbed onto the surface of the PBA particles. Finally, PBA/silica/PMMA core–shell composite latex particles were successfully prepared by two-step emulsion polymerization using PBA/silica composite particles as the seeds. Silica particles were effectively embedded in the organic phase through *in situ* "grafting" polymerization of MMA from PBA/silica seeds.

## References

1. Caris, C. H. M.; Elven, L. P. M.; Herk, A. M.; German, A. L. Br Polym J 1989, 21, 133.
2. Wu, K. H.; Chang, T. C.; Wang, Y. T.; Chiu, Y. S. J Polym Sci, Part A: Polym Chem 1999, 37, 2275.
3. Sondi, I.; Fedynyshyn, T. H.; Sinta, R.; Matijevic, E. Langmuir 2000, 16, 9031.
4. Tissot, I.; Novat, C.; Lefebvre, F.; Bourgeat-Lami, E. Macromolecules 2001, 34, 5737.
5. Fleming, M. S; Mandal, T. K.; Walt, D. R. Chem Mater 2001, 13, 2210.
6. Yang, Z. Z.; Qiu, D.; Li, J. Macromol Rapid Commun 2002, 23, 479.
7. Furusawa, K.; Kimura, Y.; Tagawa, T. J Colloid Interface Sci 1986, 109, 69.
8. Bourgeat-Lami, E.; Espiard, P.; Guyot, A. Polymer 1995, 36, 4385.
9. Espiard, P.; Guyot, A. Polymer 1995, 36, 4391.
10. Espiard, P.; Guyot, A. Polymer 1995, 36, 4397.
11. Zhang, K.; Chen, H. T.; Chen, X.; Chen, Z. M.; Cui, Z. C.; Yang, B. Macromol Mater Eng 2003, 288, 380.
12. Hajji, P.; David, L.; Gerard, J. F.; Pascault, J. P.; Vigier, G. J Polym Sci, Part B: Polym Phys 1999, 37, 3172.
13. Kaddami, H.; Gerard, J. F.; Hajji, P.; Pascault, J. P. J Appl Polym Sci 1999, 73, 2701.
14. Hayashi, S.; Fujiki, K.; Tsubokawa, N. React Funct Polym 2000, 46, 193.
15. Carrot, G.; Diamanti, S.; Manuszak, M.; Charleux, B.; Vairon, J.-P. J Polym Sci, Part A: Polym Chem 2001, 39, 4294.
16. Barthet, C.; Hickey, A. J.; Cairns, D. B.; Armes, S. P. Adv Mater 1999, 11, 408.
17. Percy, M. J.; Barthet, C.; Lobb, J. C.; Khan, M. A.; Lascelles, S. F.; Vamvakaki, M.; Armes, S. P. Langmuir 2000, 16, 6913.
18. Bourgeat-Lami, E.; Lang, J. J Colloid Interface Sci 1998, 197, 293.
19. Bourgeat-Lami, E.; Lang, J. J Colloid Interface Sci 1999, 201, 281.
20. Luna-Xavier, J. L.; Bourgeat-Lami, E.; Guyot, A. Colloid Polym Sci 2001, 279, 947.
21. Luna-Xavier, J. L.; Guyot, A.; Bourgeat-Lami, E. J Colloid Interface Sci 2002, 250, 82.
22. Luna-Xavier, J. L.; Guyot, A.; Bourgeat-Lami, E. Polym Int 2004, 53, 609.
23. Zhou, S. X.; Wu, L. M.; Sun, J.; Shen, W. D. Prog Org Coat 2002, 45, 33.
24. Wu, R. D.; Tong, X. L.; Shen, Y. L.; Wang, R. L. China Plastics (in Chinese) 2002, 16, 55.
25. Briggs, T. R. Ind Eng Chem Prod Res Dev 1921, 13, 1008.